Analysis of a Vapor-Cell Magneto-Optical Trap for Sodium Atoms Based on a Two-Level Doppler Theory

D. M. B. P. Milori, M. T. de Araujo, I. Guedes,
S. C. Zilio and V. S. Bagnato

Departamento de Física e Ciência dos Materiais, Instituto de Física de São Carlos - USP,
Caixa Postal 369, 13560-970, São Carlos, SP, Brazil

Received June 14, 1996. Revised form December 13, 1996

We present an experimental study to characterize a sodium vapor-cell magneto-optical trap (VCMOT) in terms of the number and density of trapped atoms, loading rate and loading time. We have investigated how these quantities change with the vapor temperature, magnetic-field gradient and laser intensity. The results obtained are explained with a simple model that employs the Doppler theory. Good agreement is obtained for most of the experimental data. Investigations on the size of the cloud as a function of the trap external parameters are also carried out. The information MOT in order to obtain the maximum presented here is useful in optimizing the number and density of trapped atoms, normally required for experiments of atomic collisions and Bose-Einstein condensation.

I. Introduction

The vapor-cell magneto-optical trap (VCMOT) is the most efficient atomic trap created so far. It can produce cold samples of atoms in an inexpensive and simple manner. Despite the popularity of the VCMOT, there has been few published results about its characterization and how to obtain the optimum operating condition.[1] The general behavior for the number and density of atoms as a function of the trap external parameters (vapor temperature, magnetic field gradient, laser detuning and laser intensity) is an useful knowledge since it determines the possible applications for those trapped atoms. For the case of Na, trapping can be achieved in two different tuning conditions, creating a unique situation with respect to other alkalis.

The behavior observed in a VCMOT can be explained with several degrees of sophistication. The simplest model is based uniquely on the spontaneous radiative force that arises from the momentum transferred to a two-level atom during the photon absorption and is normally referred to as the Doppler theory.[2] Other more complete theories have been established[3] and created additional tools, not present in the Doppler theory. Among these improvements, the existence of sub-Doppler temperatures is the most studied so far.[4] Manifestations of sub-Doppler mechanisms in the spring and damping constants have also been reported and investigated.[5–7] For a large number of atoms in the trap one must also take into account the existence of a secondary scattering radiation force[8,9] which prevents the density to increase.

In this work we have carried out a characterization of a VCMOT operating with sodium atoms. One can optimize the trap operation by observing how it behaves as variations are introduced to the external parameters. We have been able to explain some of the observed behavior using the Doppler theory or one of its variants. This work starts by presenting the main ideas of the VCMOT operation, followed by the description of our own experimental setup. The two traps originated from different laser tuning conditions are then discussed. The loading time, trap size, number of trapped atoms and atomic density are individually investigated as function of external parameters for the trap operation. When strong restrictions do not apply, explanations are provided by use of the Doppler theory

or one of its variants.

II. The vapor-cell magneto optical trap (VCMOT)

Although the basic concepts involved in trapping atoms have already been discussed extensively, some of the main features will be given here for the sake of completeness. If an atom with a F (total angular momentum) ground state and a $F+1$ excited state is placed in a region with a magnetic field $B(z) = B_0 z$, the Zeeman shifts on both states becomes spatially dependent. Light with a given polarization state will interact with the atom differently for different positions, mainly due to the Zeeman splitting and selection rules for the transitions. Two counter-propagating light beams, with opposite circular polarizations and red tuned from the zero-field resonance, exert a force on the atom given by[10]

$$F_z = 2\Gamma\hbar k \frac{s\delta}{(1+s)^2\left(\delta^2 + \frac{\Gamma^2}{4}\right)}\left(k\frac{dz}{dt} + z\frac{d\omega}{dz}\right) \qquad (1)$$

where $\hbar$ is the reduced Planck's constant, k is the amplitude of the wave-vector, Γ is the natural linewidth of the transition, $s = (\Omega^2/2)/(\delta^2 + \Gamma^2/4)$ is the saturation parameter for a Rabi frequency Ω, δ is the laser detuning from the atomic resonance and $(d\omega/dz)$ is the variation of the resonance frequency on the space. Eq.(1) represents a damped harmonic force whenever $\delta < 0$. When we have three pairs of mutually orthogonal laser beams, similar equations for x and y directions are obtained.

In an atomic vapor, atoms with velocities small enough can be captured and remain trapped. If the loading overcomes the losses due to collisions with fast atoms we have a net accumulation. The evolution for the number of trapped atoms obeys fhe equation[2]:

$$\frac{dN}{dt} = L - N\gamma - \beta\frac{N^2}{V_t} \qquad (2)$$

where L is the loading rate, γ is the rate of losses due to collisions with hot atoms in the vapor, β is the loss rate due to collisions involving trapped atoms and V_t is the volume occupied by the trapped atoms. For small N, the last term is negligible due to the low rate of binary collisions within the trap.

If we assume that all atoms entering into the capture volume (defined by the intersection of all laser beams) with speeds bellow v_c (capture velocity) will be trapped, one can develop a simple kinetic model for L. Considering a Maxwell-Boltzmann distribution for the vapor, a straightforward calculation leave us with[8]:

$$L = 0.67 n_{Na} V^{2/3} v_c^4 \left(\frac{m}{2K_B T}\right)^{2/3} \qquad (3)$$

where n_{Na} is the density of sodium in the vapor, m is the atomic mass, T is the vapor temperature, K_B the Boltzmann's constant and V is the capture volume.

The loss rate due to collision with hot atoms in the vapor can be determined by considering that we have mainly Na and N_2 in the vapor. Nitrogen is the residual gas (determined with a mass analyzer connected to the vacuum chamber). In this case:

$$\gamma = (n_{Na}\sigma_{Na-Na}\bar{v}_{Na} + n_{N_2}\sigma_{Na-N_2}\bar{v}_{N_2}) \qquad (4)$$

where σ_{Na-Na} and σ_{Na-N_2} are the cross-sections for elastic collisions among the species specified by the subscripts and $v = \sqrt{8K_BT/m}$ is the average atomic velocity in the vapor. Both cross sections have been previously measured[11,12] having the values $\sigma_{Na-Na} = 100 \cdot 10^{-14}$ cm^2 and $\sigma_{Na-N_2} = 3.3 \cdot 10^{-14}$ cm^2.

The volumetric loss rate β has been measured for Na as a function of the laser density[7] but is not important for the present study since we have worked in a regime where collisions with the background vapor predominates.

III. Experimental setup

Our apparatus is similar to those already described by others authors.[9,11] The VCMOT is formed by the sodium vapor contained in a stainless steel cell with several windows. The laser beam generated from a ring dye laser passes through a home-made electro-optic modulator which introduces sidebands at 1.712 GHz from the carrier frequency. The beam is then divided in three arms with equal intensities in order to produce the incident trapping beams in three orthogonal directions. After passing through the cell the beams are retro-reflected, forming counter-propagating pairs in each direction. The existence of quarter-wave plates

before and after passing through the cell guarantees opposite circular polarizations of the counter-propagating beams. All optical elements have anti-reflector coating to avoid intensity imbalance between the two counter-propagating beams.

The laser frequency is near resonant with the transition $3S_{1/2}(F = 2) \rightarrow 3P_{3/2}(F = 3)$. The blue sideband is resonant with the $3S_{1/2}(F = 1) \rightarrow 3P_{3/2}(F = 2)$ transition and works as a repumper, recovering population for the $3S_{1/2}(F = 2)$ state. The magnetic field is produced by a pair of coils placed along one axis and carrying opposite currents. This produces a spherical quadrupole field whose gradient at the center can vary from zero to 25 G/cm. Electrical heating tapes and thermocouples allow the control of the cell temperature. An ion pump keeps the background pressure below 10^{-8} Torr. The number of trapped atoms is measured by imaging the fluorescence of the trapped cloud onto a calibrated photomultiplier tube. The number of trapped atoms is proportional to the total fluorescence, with a proportionality constant given by the power-broadened scattering rate which depends on the laser detuning and intensity. The volume of the cloud is measured by using the image obtained with a video camera and a survey telescope with resolution better than 0.1 mm. Once the number of trapped atoms and the volume of the cloud are known, the density can be easily determined by taking the ratio between them. The loading time of the trap can be measured by the time evolution of the fluorescence just after opening the trapping laser. A scheme of the apparatus is presented in Fig. 1.

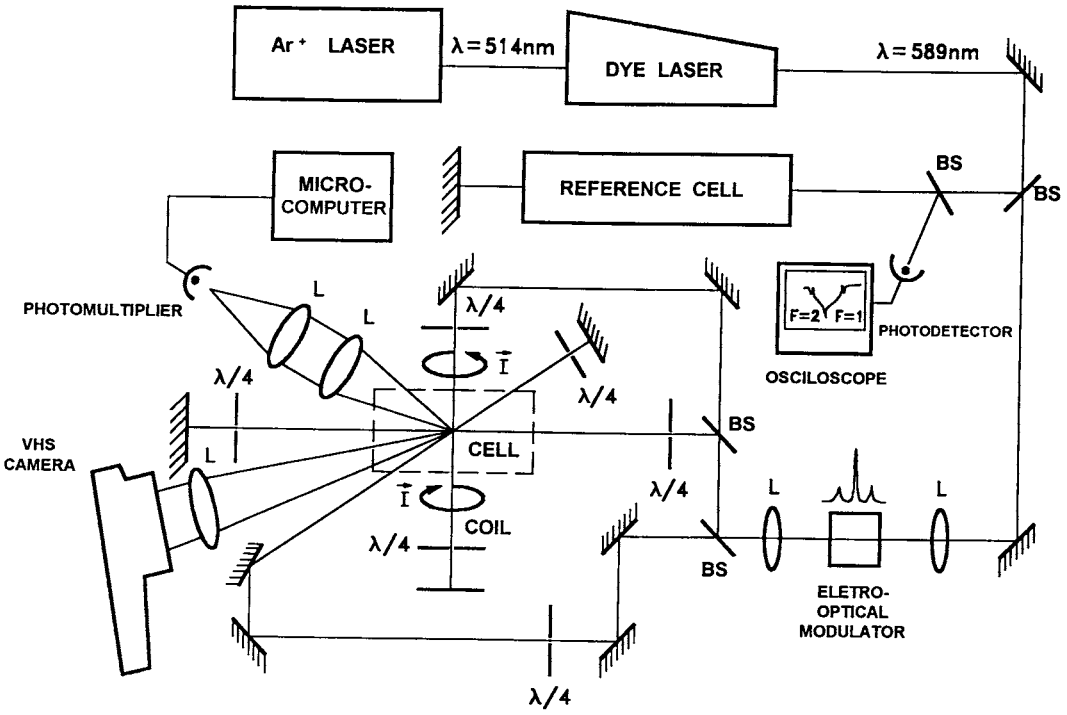

Figure 1. Experimental setup of the vapor-cell magneto-optical trap.

IV. Results and discussions

a) Tuning conditions for trapping sodium atoms

Trapping of sodium atoms can be achieved for two tuning conditions which can be obtained by scanning the laser frequency and recording the fluorescence. The result of the number of trapped atoms as a function of laser frequency is presented in Fig.2 and the correspondent combinations of transitions are shown in Fig.3. Type I trap occurs when the laser frequency is near resonant with the $3S_{1/2}(F = 2) \rightarrow 3P_{3/2}(F = 3)$ and

the sideband (repumper) is resonant with $3S_{1/2}(F = 1) \rightarrow 3P_{3/2}(F = 2)$. Type II trap occurs when the laser and sideband are tuned 60 MHz to the red of type I tuning condition. The two traps are very different in shape and number of atoms, with type I being more dense than type II. Fig.4 shows images of both traps as recorded by our video camera. Trap II has the main characteristic of being larger in number and size than type 1, but lower in density. We have systematically investigated the behavior of both trap types on several external parameters but in what follows we will present results mainly for the type I trap, which is the most interesting for several kinds of studies due to its higher density.

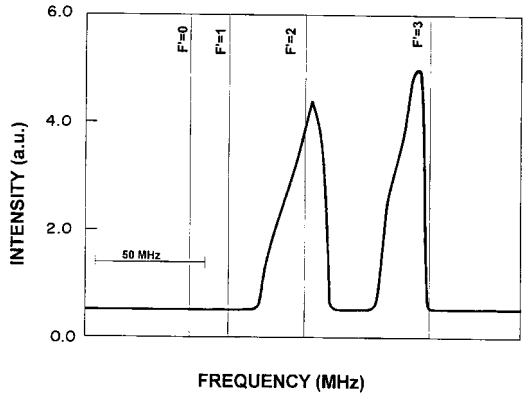

Figure 2. Fluorescence as a function of the laser frequency for type I and type II tuning conditions. The vertical lines represent the positions of the hyperfine levels of the transition $3S_{1/2}(F = 2)$ to $3P_{3/2}$.

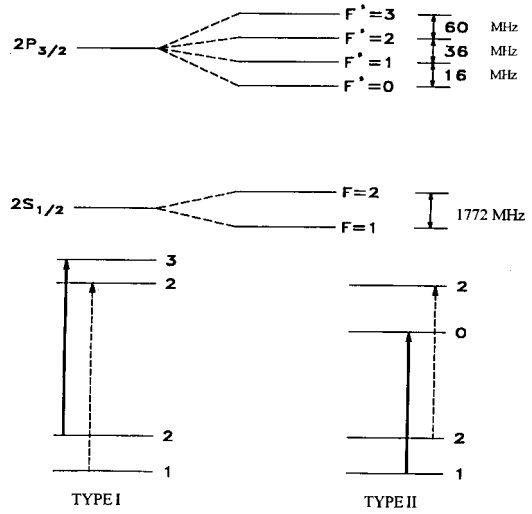

Figure 3. Energy levels of sodium and transitions involved in type I and type II tuning conditions. Solid and dashed arrows represent respectively the carrier and sideband frequencies.

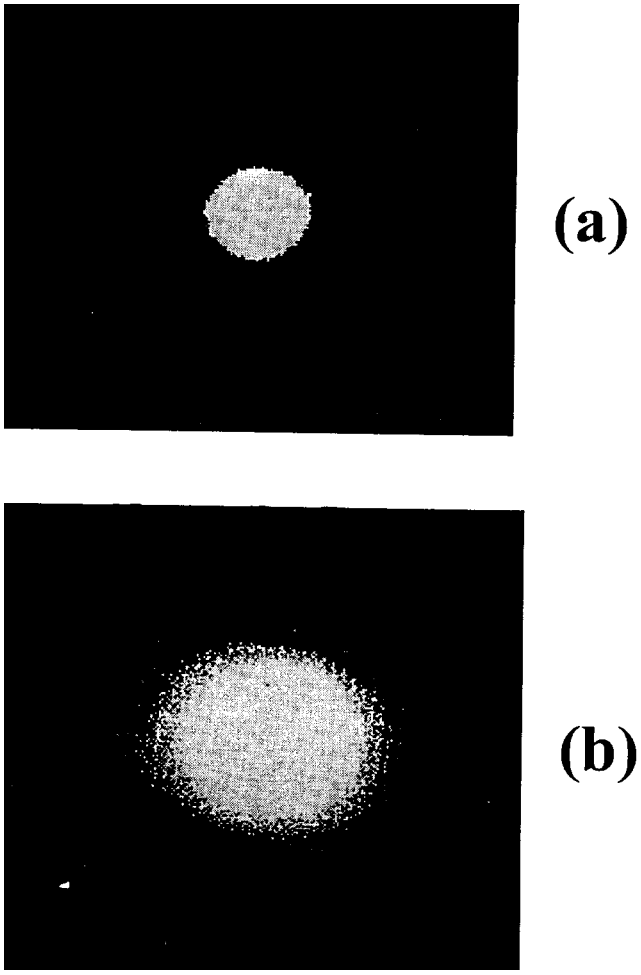

Figure 4. Images of spatial distribution of sodium atoms trapped in a VCMOT for (a) type I and (b) type II tuning conditions.

b) Dependence on the temperature

At earlier stages of the loading process N is small and the term β in Eq. (2) can be neglected. In this case, the number of trapped atoms evolves as a simple exponential with a time constant $\tau(N = N_0(1-\exp(-t/\tau))$, with $\tau = \gamma^{-1}$. We measured the loading time as a function of the vapor temperature and the result is presented in Fig. 5(a). The decrease of τ with the vapor temperature is a consequence of variations on the average velocity and density of the sodium vapor appearing in Eq. (4). A simple model can be employed by considering the foreign N_2 gas as ideal, with a fixed number of atoms inside the cell and with the Na vapor obeying the law given by:

$$n_{Na} = \frac{Ae^{BT}}{T} \qquad (5)$$

The experimental data of Fig. 5(a) can be fitted by Eq. (4), as shown by the solid line, when the values $A = 4.810^8$ K/m^3 and $B = 0.045$ K^{-1} are used in Eq. (5). This simple model confirms the fact that the decrease of the loading time with the temperature is a consequence of the increase in the rate of collisions of trapped atoms with untrapped hot atoms.

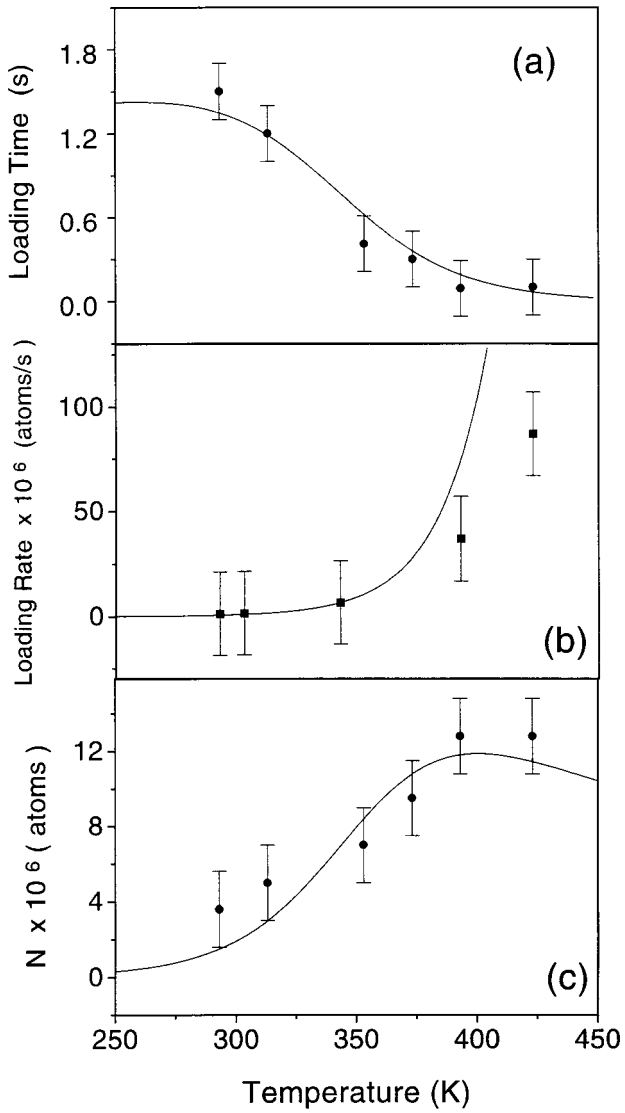

Figure 5. Temperature dependence of (a) loading time, (b) loading rate and (c) steady-state number of atoms for the type I trap in a sodium VCMOT, operating with a magnetic field gradient of 20 G/cm, detuning of 10 MHz and a laser intensity of 40 mW/cm^2 for each beam. The points correspond to the experimental data while solid curves are theoretical fittings described in the text.

The loading rate given by Eq. (3) can be measured by monitoring the number of trapped atoms at earlier stages of the loading process ($t < \tau$). In this case $N(t)$ is very small and can be neglected in Eq. 2 such that, the initial growth rate of the fluorescence gives the value of L. The observed loading rates as a function of vapor temperature are presented in Fig. 5(b). The increase of L with the vapor temperature is a consequence of the larger number of atoms with velocities below v_c. The loading rate is proportional to the sodium density and if we use Eq. (5) in Eq. (3) we introduce an exponential dependence of the loading rate with the temperature. Using this assumption, the theory fits the experimental data for a reasonable range of temperatures, as presented by solid line in Fig. 5(b).

In order to obtain the number of trapped atoms, the bright spot of the trap is imaged into a calibrated photomultiplier tube. The number of atoms we refer here is the one obtained in the steady-state operation ($dN/dt = 0$) which is, in a first approximation, the product $L\tau$. Experimental results for N as a function of the vapor temperature is shown in Fig. 5(c). This data reproduces well the expected behavior of the product $L\tau$. At low temperatures, the number is limited by the small loading rate while for higher temperatures, the compromise between the increasing in both the loading and the collision rates (decrease in τ) takes to a more or less constant value for N of about 10^7 atoms. The simple model based on the Doppler theory predicts well this result as shown by the solid line of Fig. 5(c).

We have also studied the dependence of the atomic density on the vapor temperature. We measured the size of the cloud of trapped atoms by using a survey telescope and a charge-coupled device (CCD) camera. The trap shape has small irregularities and we have averaged them by considering a mean radius. The finite size of the trap is a consequence of two features: first, the finite temperature of the cloud, causing a distribution of atoms along the potential well. Second, if the sample is dense enough, secondary photon scattering causes repulsion between atoms introducing a size, even for $T = 0$. [8] The density was estimated by taking the ratio between the number of trapped atoms and the cloud volume. This information is interesting for the purpose of observing cold collisions, collective effects such as Bose-Einstein condensation and nonlinear optical properties of trapped atoms. As the loading rate is enhanced by the vapor temperature increase, the density also increases while the cloud radius stays the same up to 390 K. After this, both the number of

atoms and the cloud radius grow at the same rate such that the density evolves to constant value. This fact is well observed if the density is plotted against the number of atoms, as shown in Fig. 6. The suration for numbers higher than 2×10^6 atoms can be explained as being due to secondary photon scattering. At usual operating conditions we work below this limit to avoid collisions with untrapped atoms.

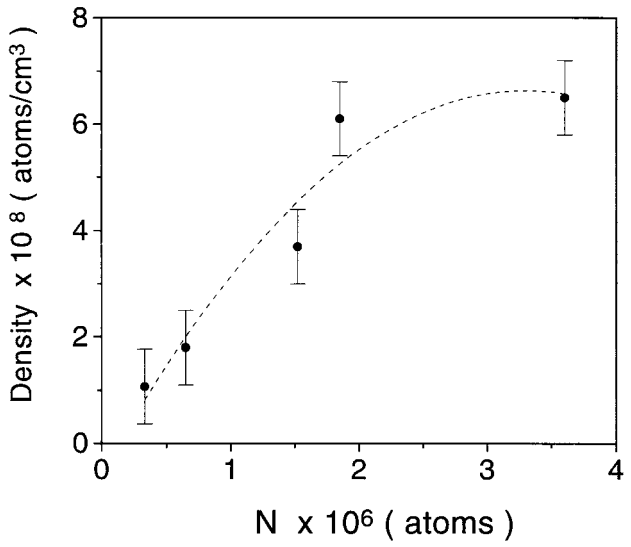

Figure 6. Density as a function of the number of atoms trapped in the type I tuning condition showing the initial linear increase and the saturation due to the radiation trapping force. The magnetic field gradient, the detunig and the laser intensity are the same as those of Fig. 5. The dashed curve is just for a visual aid.

c) Dependence on the magnetic field gradient

The behavior of the loading time, loading rate and number of trapped atoms as a function of the axial magnetic field gradient are presented in Fig. 7. As the field gradient increases, the loading time decreases until it reaches a minimum at 25 G/cm, as shown in Fig. 7(a). The reason for this is due to the fact that as the field gradient grows, the number of atoms and density increase, as presented in Fig. 7(c), and collisions between trapped atoms can not be neglected. It contributes to the transient behavior reducing the loading time. Although we believe that this is the main reason, other effects such as the trap depth and variations of the spatial selection rules also contribute to this behavior.

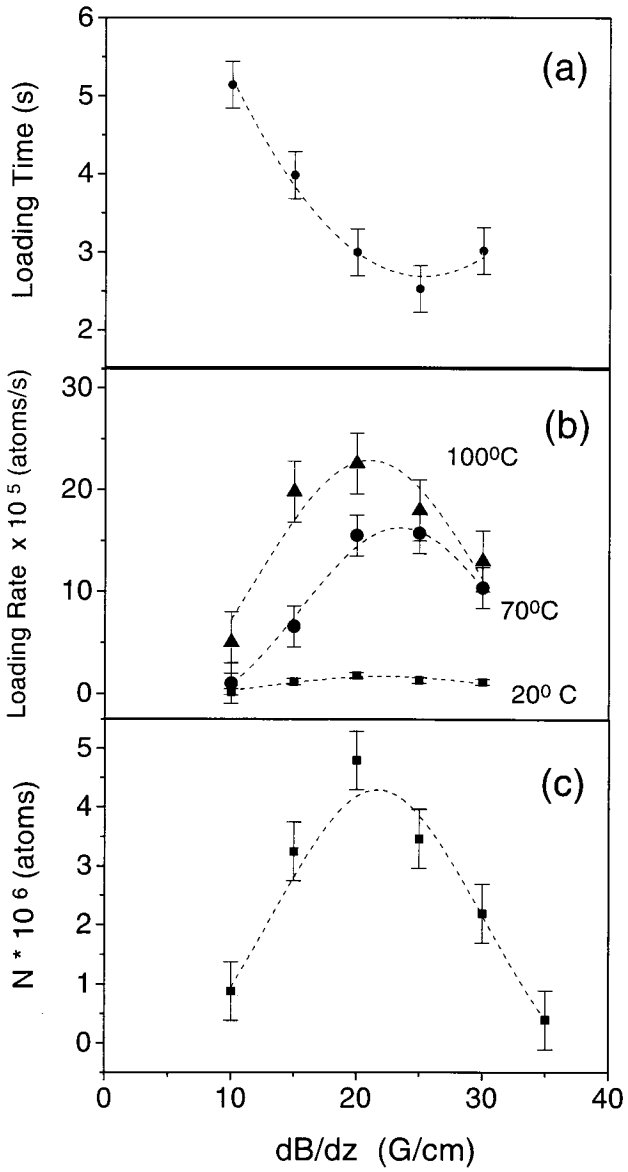

Figure 7. Magnetic field gradient dependence of (a) loading time, (b) loading rate and (c) steady-state number of atoms for the type I trap in a sodium VCMOT, operating with a laser intensity of 40 mW/cm^2 for each beam and detuning of 10 MHz. In (a) and (c) the temperature is 70°C. The curves are just for visual aid.

The loading rate as a function of field gradient presents a maximum at about 20 G/cm, as shown in Fig. 7(b). This behavior illustrates the importance of the magnetic field in the capture process of atoms in a VCMOT. The capture volume has a characteristic length of 1 cm. Across this distance, atoms are decelerated and captured by the radiation force. If the field has a high gradient inside the capture range, atoms are Zeeman tuned out of resonance and can not stay resonant along the deceleration path, causing a decrease in the loading rate. In other words, they cannot follow

the magnetic field adiabatically. For the sodium case, $\mu(dB/dz)\Delta z \sim 2\Gamma$ represents the tolerable field variation. Considering $\Delta z \sim 0.7$ cm, $\mu \sim 2\pi \times 1.4$ MHz/G, $\Gamma \sim 2\pi \times 10$ MHz we obtain (dB/dz) 20 G/cm as the maximum. Gradients above this value will make atoms to be almost out of resonance at the boundary of the capture volume, causing a decrease in the loading process. Fig. 7 (c) shows the dependence of the number of atoms on the magnetic field gradient, which follows roughly the product $L\tau$.

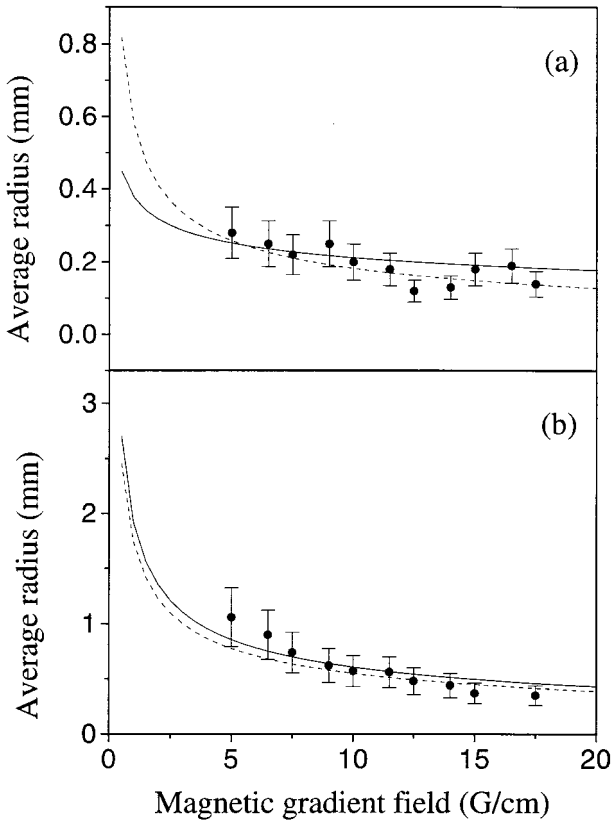

Figure 8. Dependence of the average radius on the magnetic field gradient for (a) type I and (b) type II tuning conditions in a sodium VCMOT, operating with a temperature of 70°C, a detuning of 10 MHz and a laser intensity of 40 mW/cm^2 for each beam. The points correspond to the experimental data. The dashed curve is a theoretical fitting with the simple two-level system Doppler model, while the solid curve takes into account all possible transitions involving Zeeman sub-levels.

Concerning to the size of the cloud, we have studied its dependence on the magnetic field gradient for both types of traps. For the interpretation of the results shown in Fig. 8 we used the Doppler model with two degrees of difficulty. First, we used a simple two-level model where $K_{\min}$, the minimum kinetic temperature, is calculated and the radius $< r^2 >$ is evaluated from $< r^2 >= 2K_{\min}/\kappa$, where κ is the spring constant, which can be obtained from Eq. (1). The result for $< r^2 >$ is[2]:

$$< r^2 >= \frac{3\pi\hbar\Gamma}{g\mu_B \left(\frac{dB}{dz}\right) k}(1+s)^4 \frac{\left(\delta^2 + \frac{\Gamma^2}{4}\right)}{2s\delta^2\Gamma^2} \qquad (6)$$

where s is the saturation parameter of the transition considered. Eq. (6) agrees with the one derived by Steane et al[2] in the limit of low intensity ($s \ll 1$). In a second level of difficulty we still use the Doppler theory but we take into account all possible transitions involving the Zeeman sub-levels of $3S_{1/2}(F = 2)$ and $3P_{3/2}(F = 3)$. In this case, different transition probabilities must be used and different probe frequencies for each pair of levels are necessary[3]. The net result is that the trapping spring and damping constant, and the minimum kinetic temperature are now sums involving all allowed transitions. The result for the trap radius using this second approximation is also presented in Fig. 8 . For the various values of the radius as a function of field gradient both models predict the observed behavior with slight variations. The decrease of radius with the increase in (dB/dz) is mainly a consequence of compressing the cloud with a higher restoring force.

d) Dependence on the laser intensity

Fig. 9 presents the loading dependence on the laser intensity. The loading time first decreases with the intensity, as shown in Fig. 9(a). We believe that this is due to the increase of the excited state population which also increases the losses arising from collisions between excited and ground state atoms. On the other hand, the loading time increases for intensities higher than 50 mW/cm^2 due to the decrease in density as consequence of the higher volume shown in Fig. 10(a). Smaller densities give rise to small collision rates and to longer loading times. The behavior of the loading rate as a function of light intensity is shown in Fig. 9(b). According to Eq. (1), the trapping force at low intensities grows linearly with the laser intensity. This fact enables the capture of atoms with larger velocities, which increases the capture velocity and causes an enhancement of the loading rate in accordance to Eq. (3). The saturation is a consequence of reaching the point where all available atoms present in the vapor are in

condition of being captured. This is confirmed by the fact that at large temperatures the saturation happens at higher levels. The final decrease for higher power may be a consequence of the influence of light shifts on the capture process. Accordingly, the steady-state number of atoms, presented in Fig. 9(c), is given as the product of L and τ, as before.

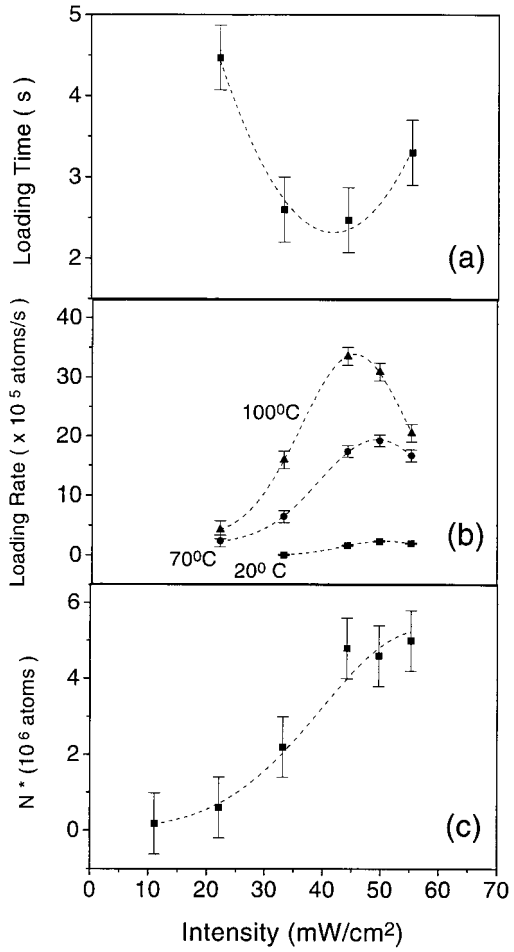

Figure 9. Intensity dependence of (a) loading time, (b) loading rate and (c) steady-state number of atoms for the type I trap in a sodium VCMOT, operating with a magnetic field gradient of 20 G/cm and a detuning of 10 MHz . The laser intensity shown in the figure is for each beam. In (a) and (c) the temperature is 70°C. The points correspond to the experimental data while dashed curves are only a visual aid.

The variation of the radius with the light intensity, given in Fig. 10, shows an initial decrease which agrees well with the simple two-level model corresponding mainly to an increase of the restoring force, which for low intensity is proportional to the light intensity. As the intensity increases, this behavior changes and the radius starts to increase with the light intensity. For this second part, the behavior seems to be in agreement with the second model where a sum over all possible transition is taken into account. Although we have not considered the radius increase with intensity in our model, it can also be a consequence of the existence of radiation trapping in the cold atomic sample generating a secondary scattering force which prevent atoms to get closer.[13–15] This result is supported by a slight tendency of the trap in staying with constant density (N increases at the same rate as the volume). However, at the density values that we usually operate the VCMOT, this seems to be a second order effect. Similar measurements and model were carried out for the type II trap, but the variations with liqht intensity does not agrees with any simple model.

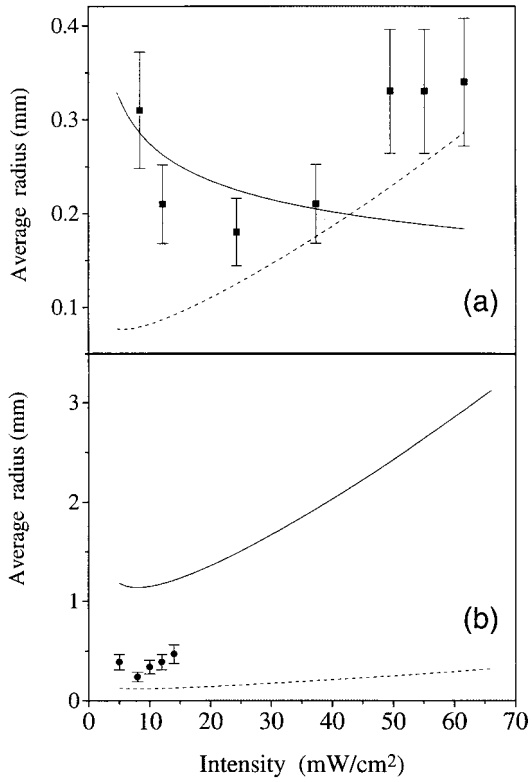

Figure 10. Dependence of the average radius on the intensity for (a) type I and (b) type II tuning conditions in a sodium VCMOT, operating with a temperature of 70°C, a detunig of 10 MHz and a magnetic field gradient of 20 G/cm. The points correspond to the experimental data. The dashed curve is a theoretical fitting with the simple two- level system Doppler model, while the solid curve takes into account all possible transitions involving Zeeman sublevels.

V. Conclusions

With the present characterization we conclude that there is a strong dependence of the number and density

of trapped atoms in stationary state on the magnetic field gradient, trapping laser intensity and sodium cell temperature. Therefore, the conditions used to operate the trap must be chosen in accordance with the specific application of the cold atoms sample. As an example, for the study of cold collisions through the production of Na_2^+ ions, the sample of trapped atoms must be dense and therefore the MOT must be working with the maximum loading rate and the minimum loss rate. In our apparatus, this point occurs for a magnetic gradient field of 20 G/cm in the z-direction, trapping laser intensity of approximately eight times the sodium saturation intensity ($I \sim 48$ mW/cm^2) and with a cell temperature of about 100°C (373K).

On the other hand, for the purpose of studying the properties of the trap, such as the measurement of the damping and restoring constants, we must work in a regime with a minimum interaction among trapped atoms. In this case, the trapping potential well must be shallow. Thus, the MOT of sodium atoms must operate in low intensities ($I \leq I_0$) and low magnetic field gradients ($\partial B/\partial z \sim 10$ G/cm). Under these conditions, and keeping the cell at room temperature, the number of trapped atoms is reduced by a factor of four, approximately. We could improve this by reducing the cell temperature. In this way, we can reduce efficiently the loss rate without changing significantly the loading rate.

In conclusion, the study presented here can be used as a guide for the construction of a MOT of sodium. However, its final characteristics are dependent on each specific system and can vary from apparatus to apparatus, according to their initial vacuum conditions.

Acknowledgments

This work was supported by FAPESP (Fundação de Amparo à Pesquisa do Estado de São Paulo), CNPq (Conselho Nacional de Pesquisas) and FINEP (Financiadora de Estudos e Projetos).

References

1. K. Lindquist, M. Stephens and C. Wieman, Phys. Rev. A **46**, 4082 (1992).
2. A. M. Steane, M. Chowdhury and C. J. Foot, J. Opt. Soc. Am. B**9**, 2142 (1992).
3. D. W. Sesko, T. G. Walker and C. E. Wieman, J. Opt. Soc. Am. B **8**, 946 (1991).
4. J. Dalibard and C. Cohen-Tannoudji, J. Opt. Soc. Am. B **6**, 2023 (1989).
5. P. D. Lett, R.N. Watts, C. I. Westbrook, W. D. Phillips, P. L. Gould and H. Metcalf, Phys. Rev. Lett. **61**, 169 (1988).
6. P. Kohns, P. Buch, W. Süptitz, C. Csambal and W. Ertmer, Europhys. Lett. **22**, 517 (1993).
7. L. G. Marcassa, V. S. Bagnato, Y. Wang, C. Tsao, J. Weiner, O. Delieu, Y. Band and P. Julienne, Phys. Rev. A **47**, R4563-6 (1993).
8. C. Monroe, W. Swann, H. Robinson and C. Wieman, Phys. Rev. Lett. **65**, 1571 (1990).
9. C. D. Wallace, T. P. Dinnenn, K. Y. N. Tan, A. Kumara Krishnan, P. L. Gould and J. Javanainen, J. Opt. Soc. Am. B **11**, 703 (1994).
10. R.J. Cook, Phys. Review A **20**, 224 (1979)
11. M. Prentiss, A. Cable, J. E. Bjorkholm, S. Chu, E. Raab and D. Pritchard, Opt. Lett. **13**, 452 (1988).
12. A. Cable, M. Prentiss and N. Bigelow, Opt. Lett. **15**, 507 (1990).
13. C. Monroe, W. Swann, H. Robinson and C. Wieman, Phys. Rev. Lett. **65**, 1571 (1990).
14. T. Walker, D. Sesko and C. Wieman, Phys. Rev. Lett. **64**, 408 (1990)
15. K. Molmer, Phys. Rev. A **44**, 5820 (1991).